Interferometric identification of ion acoustic broadband waves in the auroral region: CLUSTER observations

M. Backrud, A. Tjulin, A. Vaivads, M. André, A. Fazakerley

Interferometric identification of ion acoustic broadband waves in the auroral region: CLUSTER observations

M. Backrud,[1,2] A. Tjulin,[3] A. Vaivads,[1] M. André,[1,2] and A. Fazakerley[4]

Received 7 February 2005; revised 21 August 2005; accepted 9 September 2005; published 15 November 2005.

[1] We determine the phase velocity and **k** vector for parallel and oblique broadband extremely low frequency, ELF, waves on nightside auroral magnetic field lines at altitudes around 4.6 R_E. We use internal burst mode data from the EFW electric field and wave instrument onboard the Cluster spacecraft to retrieve phase differences between the four probes of the instrument. The retrieved characteristic phase velocity is of the order of the ion acoustic speed and larger than the thermal velocity of the protons. The typical wavelength obtained from interferometry is around the proton gyro radius and always larger than the Debye length. We find that in regions with essentially no suprathermal electrons above a few tens of eV the observed broadband waves above the proton gyro frequency are consistent with upgoing ion acoustic and oblique ion acoustic waves.
Citation: Backrud, M., A. Tjulin, A. Vaivads, M. André, and A. Fazakerley (2005), Interferometric identification of ion acoustic broadband waves in the auroral region: CLUSTER observations, *Geophys. Res. Lett.*, *32*, L21109, doi:10.1029/2005GL022640.

1. Introduction

[2] Broadband waves have been observed earlier by a number of satellites and rockets in the auroral region [e.g., *Gurnett and Frank*, 1977; *Wahlund et al.*, 1998; *Kintner et al.*, 2000]. Broadband extremely low frequency, ELF (from the ion gyro frequencies to the ion plasma frequency) waves are interesting because of their ability to interact with particles and therefore exchange energy between particle populations. *Bonnell et al.* [1996] used interferometry to determine the phase velocity of broadband ELF waves in the auroral ionosphere from AMICIST data. The interpretation of the rocket measurements was that the broadband emissions were electrostatic proton cyclotron waves.

[3] *Backrud et al.* [2004, 2005] used two different methods to compare wave and particle observations with theory to identify the wave modes in the observed broadband waves between 10 and 180 Hz. Both methods used the observed wave polarization and compared it with the polarization obtained from linear theory in a homogeneous plasma. In the first method, two ratios of wave field components ($\delta E_{\parallel}/\delta E_{\perp}$ and $\delta E/\delta B$) were compared with theory and in the second method, an estimate of the distribution of energy in wave vector space using all components was performed. Both methods identified the observed broadband waves to be a mixture of ion acoustic, oblique ion acoustic and electrostatic ion cyclotron waves.

[4] In this study we use interferometry as a new, third method, to determine the wave characteristics of the observed broadband waves above the proton gyro frequency at an altitude of 4.6 R_E. The event is from Cluster spacecraft 2, 14th of February 2003, and the same event observed by Cluster spacecraft 4 is analysed in detail by different methods by *Backrud et al.* [2005]. Earlier methods identified the broadband waves to be a mixture of electrostatic ion cyclotron waves, ion acoustic and possibly also ion Bernstein waves. This study goes one step further and determines the wavelengths and the **k** vectors for the observed ion acoustic waves.

2. Observations

[5] In this study we use data from the EFW double-probe electric field and wave instrument [*Gustafsson et al.*, 1997] onboard Cluster spacecraft 2 [*Escoubet et al.*, 1997], together with observations from the PEACE electron spectrometers [*Johnstone et al.*, 1997]. The event we present in this study occurred when the EFW instrument was in internal burst mode, i.e. with a sampling-rate of 9000 samples/second.

[6] For the event of interest, the proton gyro frequency is 7.7 Hz, the proton plasma frequency is 330 Hz and the lower hybrid frequency is around 160 Hz (assuming the plasma consists of equal amounts of H^+ and O^+, measured by Spacecraft 4). The density is estimated to 5 cm^{-3} from the plasma line observed by the resonance sounder WHISPER [*Décréau et al.*, 1997] (not shown). The ion acoustic speed (with an electron temperature of 2 keV and the mass from H^+ and O^+) is estimated to be around 200 km/s, which is above the thermal speed of the protons (150 km/s for 100 eV protons). The ion species and temperatures are estimated from the CIS instrument on Cluster spacecraft 4 [see also *Backrud et al.*, 2005].

[7] Figure 1 shows an overview of the region in which the internal burst (highlighted in yellow in Figures 1a and 1b) take place. The electric field components are in Figure 1 sampled with 450 samples/second and band-pass filtered between 10 and 180 Hz. Since the ambient magnetic field is almost (<2°) in the spin plane, we can divide the observed electric field in the spin plane into one perpendicular and one parallel and neglect the third component since it is not measured component (see also *Backrud et al.* [2004] for details of the method). The parallel component (Figure 1b) is most of the time larger than the perpendicular

[1]Swedish Institute of Space Physics, Uppsala, Sweden.
[2]Department of Astronomy and Space Physics, Uppsala University, Uppsala, Sweden.
[3]Laboratoire de Physique et Chimie de l'Environnement, Centre National de la Recherche Scientifique, Orléans, France.
[4]Mullard Space Science Laboratory, London, UK.

0094-8276/05/2005GL022640

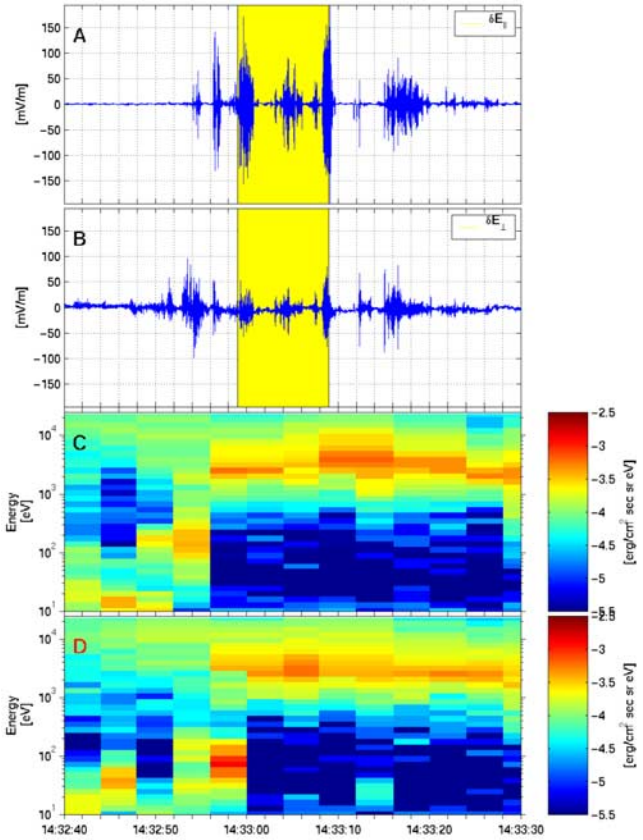

Figure 1. On overview plot showing that (b) the parallel component is larger than (a) the perpendicular component of the electric field in association with a void of suprathermal, both (c) upgoing and (d) downgoing electrons. Highlighted yellow region is internal burst mode data available and will be studied further in more detail.

component (Figure 1a) in regions with very few upgoing and downgoing electrons (Figures 1c and 1d, respectively) at energies above 10 eV. Waves with larger parallel than perpendicular component are consistent ion acoustic waves and have been observed earlier in regions with essentially no suprathermal electrons between ten and a few hundred eV [*Backrud et al.*, 2005].

[8] The broadband waves are interpreted to be of electrostatic nature [*Backrud et al.*, 2004, 2005], which implies that the waves are longitudinal with a **k** vector parallel to the wave electric field. In the highlighted yellow region in Figure 1, the EFW instrument is in burst mode and it is possible to obtain the potentials from all four probes with a sampling rate of 9000 samples/second (with a 4500 Hz low-pass filter). The probe orientation is displayed in Figure 2 where the red line is the direction of the ambient magnetic field. The arrow showing the direction of the **k**-vector will be discussed later.

[9] Internal burst mode gives us the opportunity to compare the phase differences between the two pairs of probes, p1-p3 and p4-p2 (phase difference of the electric field obtained between probe 1 and probe 3 and the electric field obtained between probe 4 and probe 2) and also between p2-p3 and p4-p1. In this method we obtain several values of the phase velocity within one wave period by correlating the steepest gradients as well as maxima and minima of the two signals. This method is used earlier on Cluster observations of lower hybrid turbulence at the magnetopause [*Vaivads et al.*, 2004].

[10] Figure 3 shows 0.7 seconds of data between 14:33:08.2–14:33:08.9 UT filtered between 40–200 Hz. Figure 3a shows the electric field derived from the signals, p13 (black line) and p23 (red line). The amplitude of the electric field derived from p23 is larger (~factor of 3) than the electric field derived from p13. Figure 3b shows the inverted parallel (black) and perpendicular (red) phase velocities for $\omega = 2\pi$?100 rad/s, which gives values of the phase velocities between 100 and 200 km/s. The $k_{\|}/k_{\perp}$ ratio varies between −1 and −2.5 (as an average between 14:33:08.45 and 14:33:08.8), which means that the waves are propagating upward with an angle φ of 21–45 degrees ($\tan(90 - \varphi) = k_{\|}/k_{\perp}$) with respect to the ambient magnetic field. The inverse of the estimated wavelength is shown in Figure 3c and the wavelengths vary between 0.5 and 3 km.

[11] From the probe orientation (Figure 2) we see that the separation vector between p2-p3 is almost parallel while p1-p3 is almost perpendicular to the ambient magnetic field. However, this is only true for this particular time displayed. During the whole interval displayed in Figure 3, the spacecraft spins approximately 60° (clockwise in the plot) and therefore the probes change their positions relative to the ambient magnetic field. The direction of the wave vector estimated from the phase velocities in Figure 3b at 14:33:08.75 ($\tan(90 - \varphi) = 0.65/0.45$) is displayed in Figure 2 (black arrow).

[12] The wave vectors obtained from this first method for the whole time interval (14:33:08.2–14:33:08.9 UT) (calculated from Figure 3 and one plotted in Figure 2) are consistent with ion acoustic waves or oblique ion acoustic waves.

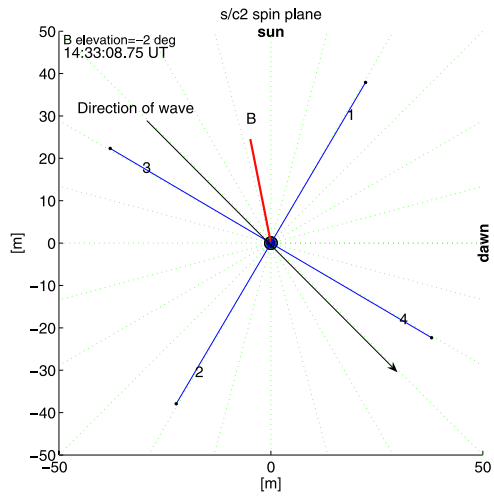

Figure 2. Displays the probe orientation (blue lines) at 14:33:08.7. Red line is the direction of the ambient magnetic field and black bold line is the propagation direction of the wave observed at this particular time. The direction is retrieved from the phase velocities. Green lines indicate angles in degrees.

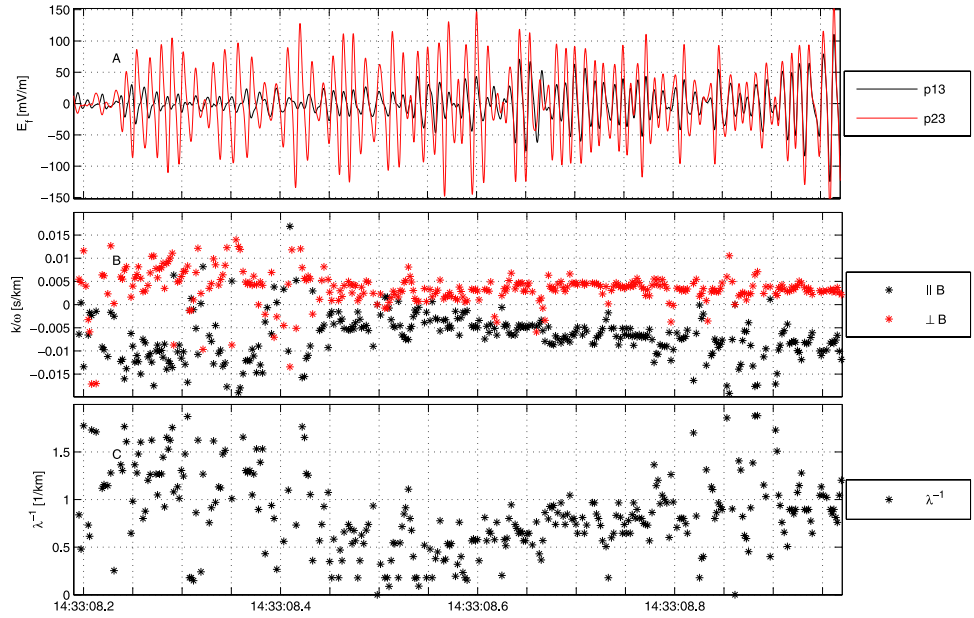

Figure 3. (a) The signal from the two probe pairs p13 (black) and p23 (red). (b) The inverse of the parallel (black) and perpendicular (red) phase velocities (see text for details) and (c) the inverse of the wavelength.

[13] In Figure 4 we have used another method, a continuous wavelet cross spectrum to estimate the phase shift between two signals between 14:33:08.7 and 14:33:08.8 UT to see how the **k** vector is changing with frequency. The data is sampled with 9000 samples/second and the frequency band displayed is between 40 and 1000 Hz. We have used the estimated phase shift between the electric fields derived from two probe pairs to calculate the projection K of the wave vector in two directions (one almost parallel and one almost perpendicular to the ambient magnetic field) as a function of frequency. The analysis we use is similar to the analysis performed by *Pincon et al.* [1997]. We assume plane waves with only one K associated with each frequency and that the wavelength is larger than the separation distance ($d = 88/2^{1/2}$) between the probes. Each time step of the wavelet analysis gives one local K-frequency spectrum, which is used to produce the wave number-frequency spectrum.

[14] The results are shown in Figure 4 where the projection of K is estimated for (a) p23-p41 and (b) p42-p13 for the frequency range 40–1000 Hz. A positive K in Figure 4a means that the wave is going from probes 2-3 to probes 4-1 while the negative K in Figure 4b means that the wave is going from probes 1-3 to probes 4-2. From Figure 3 we can see that K in Figure 4a represents an almost perpendicular component ($K_\perp$) while Figure 4b represents an almost parallel component of K ($K_\parallel$). The waves are broadbanded in the sense that they extend between 50 and 300 Hz with the most power above 60 Hz and up to the ion plasma frequency around 300 Hz. In Figure 4a, $K_\perp$ is changing linearly with frequency, which corresponds to wavelengths between 3 km (60 Hz) and 1 km (150 Hz). The estimated plasma drift is approximately 3 km/s, mainly in the z_{gse} direction, i.e. perpendicular to the spin plane and parallel to the direction of the spacecraft velocity. This implies a Doppler broadening of a few Hz at the most. In Figure 4b, $K_\parallel$ is slightly larger than $K_\perp$ and the direction of the wave is

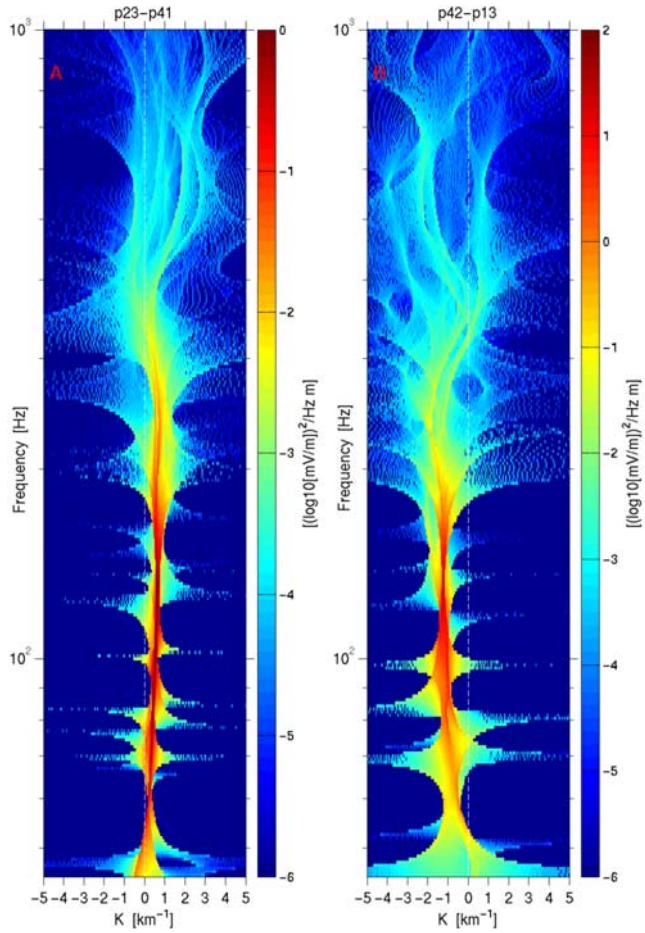

Figure 4. Local wave number frequency spectra retrieved from (a) p23-p41 and (b) p42-p13 between 14:33:08.7–14:33:08.9 UT.

consistent with the one obtained from Figure 3, and plotted in Figure 2. The phase velocity can be estimated to around 200 km/s from the slope of the K vector as a function of frequency in Figure 4b (200−40/(1.2−0.4)). This is consistent with the phase velocity estimated in Figure 3 and the observed waves are interpreted, also for this second method, to be ion acoustic or oblique ion acoustic waves.

3. Discussion and Conclusions

[15] Previous observations of broadband waves on auroral magnetic field lines at an altitude of around $4.6R_E$ have been identified as linear waves in homogeneous plasma [*Backrud et al.*, 2004, 2005]. The same author also concluded that the broadband waves are a mixture of electrostatic ion cyclotron waves, oblique ion acoustic and ion acoustic waves, i.e. waves on the same dispersion surface [*André*, 1985].

[16] We use the EFW instrument onboard the Cluster spacecraft to do an interferometric determination of the phase velocity and **k** vector of broadband ELF waves at an altitude of about 4.6 R_E in the nightside auroral region. We determine the projection of the **k** vector for broadband waves between 40 Hz and 300 Hz (covering the lower hybrid frequency and reaching up to the ion plasma frequency) in two different ways. The methods show good consistency and confirm that $|k_{\|}/k_{\perp}|$ varies between 1 and 2.5. The methods also showed that the waves are upgoing with an angle of 21−45° with respect to the ambient magnetic field, with a characteristic phase velocity of 200 km/s. This phase velocity is the same as the estimated ion acoustic speed of 200 km/s (with an electron temperature of 2 keV and the mass from equal amount of H^+ and O^+) but larger than the thermal velocity of the protons (150 km/s for 100 eV protons). The ion species and temperatures are estimated from the CIS instrument on Cluster spacecraft 4 [see also *Backrud et al.*, 2005].

[17] The wavelengths of the broadband waves in this event vary between 0.5 km and up to 3 km, which is of the same order as the proton gyro radius of 3 km (for 100 eV protons) but larger than the Debye length (150 m for $n = 5\ cm^{-3}$ and $T_e = 2$ keV).

[18] Adding this together, we can confirm previously reported results of existing ion acoustic or oblique ion acoustic waves in regions void of suprathermal electrons (a few tens to a few hundred eV) on auroral magnetic field lines at altitudes of around 4.6 R_E. New results in this event show that the ion acoustic waves are propagating upwards with an angle of a few tens of degrees and with a phase velocity of the order of the ion acoustic speed but slightly larger than the thermal velocity of the protons.

[19] **Acknowledgment.** The Swedish National Space Board (SNSB) supports the EFW instruments on board CLUSTER. CIS ion data was provided by Y. Hobara.

References

André, M. (1985), Dispersion surfaces, *Plasma Phys.*, *33*, 1−19.
Backrud, M., et al. (2004), Identification of broadband waves above the auroral acceleration region, *Ann. Geophys.*, *22*, 4203−4216.
Backrud, M., et al. (2005), Cluster observations and theoretical explanations of broadband waves in the auroral region, *Ann. Geophys.*
Bonnell, J., P. Kintner, J.-E. Wahlund, K. Lynch, and R. Arnoldy (1996), Interferometric determination of broadband ELF wave phase velocity within a region of transverse auroral ion acceleration, *Geophys. Res. Lett.*, *23*, 3297−3300.
Décréau, P. M. E., et al. (1997), WHISPER, a resonance sounder and wave analyzer: Performance and perspectives for the Cluster mission, *Space Sci. Rev.*, *79*, 157−193.
Escoubet, C. P., C. T. Russel, and R. Schmidt (1997), The Cluster and Phoenix Missions, *Space Sci. Rev.*, *79*, 1−658.
Gurnett, D. A., and L. A. Frank (1977), A region of intense plasma wave turbulence on auroral field lines, *J. Geophys. Res.*, *82*, 1031−1050.
Gustafsson, G., et al. (1997), The electric field and wave experiment for the Cluster mission, *Space Sci. Rev.*, *79*, 137−156.
Johnstone, C., et al. (1997), PEACE: A plasma electron and current experiment, *Space Sci. Rev.*, *79*, 351−398.
Kintner, P. M., J. Franz, P. Schuck, and E. Klatt (2000), Interferometric coherency determination of wavelength or what are broadband ELF waves?, *J. Geophys. Res.*, *105*, 21,237−21,250.
Pincon, J. L., P. M. Kintner, P. W. Schuck, and C. E. Seyler (1997), Observations and analysis of lower hybrid solitary structures as rotating eigenmodes, *J. Geophys. Res.*, *102*, 17,283−17,296.
Vaivads, A., M. André, S. C. Buchert, J.-E. Wahlund, A. N. Fazakerley, and N. Cornilleau-Wehrlin (2004), Cluster observations of lower hybrid turbulence within thin layers at the magnetopause, *Geophys. Res. Lett.*, *31*, L03804, doi:10.1029/2003GL018142.
Wahlund, J.-E., et al. (1998), Broadband ELF plasma emission during auroral energization 1. Slow ion acoustic waves, *J. Geophys. Res.*, *103*, 4343−4376.

M. André, M. Backrud, and A. Vaivads, Uppsala Division, Swedish Institute of Space Physics, P. O. Box 537, SE-751 21 Uppsala, Sweden. (ma@irfu.se)
A. Fazakerley, Mullard Space Science Laboratory, University College London, Surrey RH5 6NT, UK.
A. Tjulin, LPCE/CNRS, 3A avenue de la Recherche Scientifique, F-45071 Orléans, France.